Role of Gravity in the Formation of Liesegang Patterns

J. M. García-Ruiz,* D. Rondón, A. García-Romero, and F. Otálora

Laboratorio de Estudios Cristalográficos, IACT, CSIC−Universidad de Granada, Av. Fuentenueva s/n, Granada 18002, Spain

Received: November 14, 1995; In Final Form: February 26, 1996[⊗]

We report the results obtained in four different kinds of experiments designed to test the effect of gravity on the formation of Liesegang patterns. Both reacting solutions (KI and $Pb(NO_3)_2$) were gelled with agarose L. The position of the PbI_2 precipitates was determined by image analysis, and the kinetic coefficients $k_m = (X_{n+1} - X_n)/X_n$ and $k_p = (X_n/A)^{1/n}$ were obtained at different relative orientations of the gravitational field with respect to the direction of the advance of the precipitation front. We conclude that there is not an apparent influence of the gravitational forces on the kinetics of the pattern formation when it is obtained in gelled media at an agarose concentration of 1% (w/v). When the experiments were performed with agarose at 0.5% (w/v) or when one of the reacting solutions was ungelled, our tests show clearly the effect of gravity.

I. Introduction

The Liesegang phenomenon is an intermittent precipitation that occurs when two reacting solutions at concentrations far from stoichiometry are allowed to counterdiffuse.[1,2] The fact that diffusion is the mass transport mechanism linked to this phenomenon has been realized since the earlier years of this century, because two gravity-related phenomena (convective flow and sedimentation of the solid phase) are known to provoke the breaking of the laws governing the formation of the patterns. This is the reason that Liesegang patterns are usually obtained in gelled media. The tridimensional network of the solid polymeric phase forming the gel leaves a fractal distribution of pores filled by the liquid phase. Due to the small average pore size, the gel structure prevents convective mass flow while allowing the Brownian motion of ions and small clusters through the intraporous fluid phase. These phenomena may occur in other porous media, such as sedimentary rocks or biological materials, a circumstance that increases the interest in revealing the origin and properties of these structures.

To determine whether gravity alters the location and the time of formation of the successive bands or rings is of interest from a theoretical viewpoint. As pointed out by Bewersdorff et al.[3], since the effect of the gravity field on ions can be neglected, the existence of a gravitational shift must be due to the presence of clusters of colloidal size ($0.1\ \mu m < r < 10\ \mu m$), which could support the explanation of Liesegang patterns as a post-nucleation event.[4,5] The first experimental results on the influence of gravity on the formation of Liesegang rings were reported by Davies,[6] who claims that the kinetics of the pattern formation is slower when operating against gravity. As quoted by Hedges,[7] this effect might be counterbalanced by hydrostatic pressure. More recently, Kai et al.[8] have considered this problem and proposed an explanation as to why such an effect could be active. They measured the dependence of the ring position on the relative directions of the advance of the precipitation front with respect to the gravitational field. Their experiments were carried out using the reaction between KI and $Pb(NO_3)_2$ to precipitate PbI_2 and between $MgSO_4$ and NH_4OH to produce MgOH. However, quantitative relations were only reported for the first case due to experimental problems that appear when gelling NH_4OH solutions. Their experimental protocol consisted of three identical experiments in three test tubes which were arranged parallel, perpendicular, and antiparallel to the **g** vector. It was found that, for the same ring number (n), the distance $X_{n+1} - X_n$ increases in the sequence antiparallel, perpendicular, and parallel to the gravity field. This effect was observed to be clear for large values of n and also when the pattern formation is slowed down by the use of more dilute solutions. The same kind of experimental proof has been recently described by Das et al.[9,10] for the case of HgI_2 and $CuCrO_4$, but in none of these cases were statistical results reported. Finally, Zrìnyi et al.[11] reported no gravity effect on the $Cr(OH)_3$ Liesegang system.

The main problem in proving the existence of a gravitational influence comes from the difficulty of performing reproducible Liesegang experiments. There are several internal parameters which modify the spatial geometry and the time relations displayed by Liesegang patterns. The initial concentrations of reactants, the surface of the reaction front, the geometry (shape, volume, and arrangement) of the reactant sources, the nature and viscosity of the gelled media, etc., are variables which change the spatiotemporal distribution of precipitate. There are other external parameters which have been claimed to influence the geometry of the Liesegang patterns. The intensity, periodicity, and wavelength of the illumination clearly affect the pattern of silver and mercury salts,[10] and the temperature has a clear effect on the precipitation behavior of other salts such as PbI_2. The effect of the type of glass reservoir and cleaning procedures has also been pointed out. Furthermore, there are factors which are much more difficult to evaluate because they vary as precipitation progresses, such as the pH of the medium and the concentration of the by-products, the age of the gel,[12] the tensional effect on the gel structures,[13] the electric field,[14,15] and the presence of impurities. How these factors affect the complex behavior of the Liesegang patterns is still a matter of research.

The aim of this work was to study the effect of the gravitational field on the kinetics of Liesegang bands on the basis that the sensitivity of these patterns to internal and external experimental conditions could mask the experimental results. We present the results of four different tests.

* Author to whom all the correspondence should be addressed. Phone: +34-58-243360. Fax: +34-58-243384. Email: jmgruiz@goliat.ugr.es

[⊗] Abstract published in *Advance ACS Abstracts,* May 1, 1996.

S0022-3654(95)03351-X CCC: $12.00

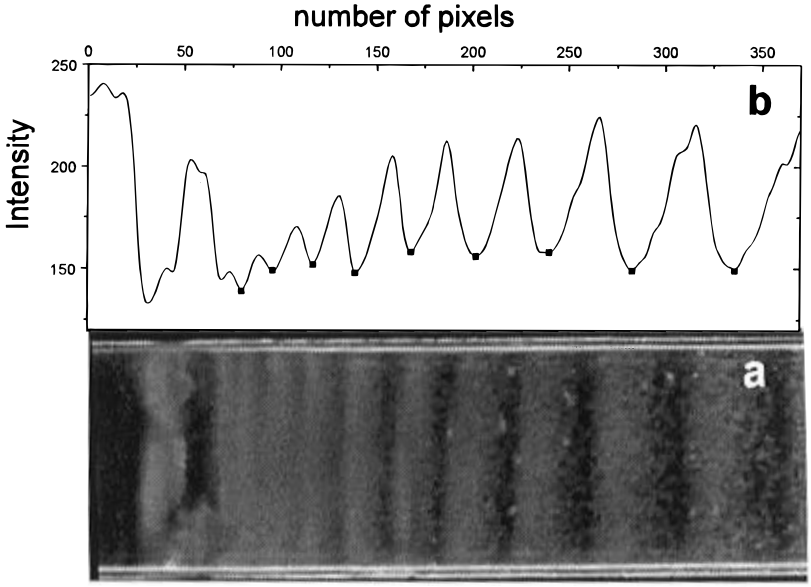

Figure 1. (a) the image stored in TIFF format once processed. (b) Determination of the ring position.

II. Experimental Section

A. Measurement of the Patterns. The ring identification procedure includes all the steps involved, from actual experiments to a list of the relative positions of the precipitates and eventually a plot of these data. Among the possible solutions to the identification problem, we select image analysis on the basis of its accuracy, rapidity, and impartiality.

The development of a Liesegang pattern is essentially dynamic, and we were forced to study the time record of these structures. Therefore, the input information used along this work was in the form of actual experiments (tubes, plates, or Petri dishes) or videotapes recording such experiments. Actual experiments were digitized by using an Epson GT6000 scanner and the Espcan software from Epson. Recorded experiments were digitized by using an E-Machines image acquisition board on a Apple Macintosh II FX and the NIH-Image software for image acquisition and Adobe Photoshop for image processing. Both procedures produce bitmaps with the desired resolution which are stored in TIFF format for further analysis. In some cases such a record was obtained using a Ricoh photographic camera with a Tamron 90 mm lens and a $\times 2$ teleconverter, but in most of the cases we also recorded the experiments by using a time lapse video recorder, Sony SVT-5000P VCR, connected to a Hitachi KPC501 Tv camera attached to a microscope. Our recordings contain the whole experiment accelerated by a factor of 60, followed by a still image 2 min long of the final stage. These videotapes were then used to take pictures using a videoprinter, to edit the images for measurement of the pattern by image analysis and to study the time evolution of the pattern.

The process of analysis starts with a filtering of the image (equalization, linearization, bright and contrast enhancement, rotations, etc.) performed by the Adobe Photoshop program in order to obtain an optimum image of the experiment (see Figure 1a). For the cases of capillary tubes and test tubes, the values of intensity are then integrated for one-dimensional experiments in the direction where no gradients are expected to obtain a signal reinforcement. By this integration we obtain a data set where $I(x)$ is the intensity averaged over all the pixels having the same x coordinates.

$$I(x) = \sum_{y=y_1}^{y_2} \mathrm{i}(x,y) \qquad (1)$$

This dataset is exported to Origin (Microcalc), where an automatic peak detection algorithm is implemented to obtain the position of the rings (maxima or minima depending on the ring/background intensity ratio), as shown in Figure 1b.

For the case of the pattern made in Petri dishes, the experiments with radial symmetry are pre-processed by a geometrical transformation that produces a polar coordinate bitmap from the Cartesian coordinates bitmap by mapping each pair of pixels.

$$I_p(x,y) = I_c\left(\frac{y}{R}Y\cos\frac{2\pi x}{X} + x_0, \frac{y}{R}Y\sin\frac{2\pi x}{X} + x_0\right) \qquad (2)$$

where $I_p(x,y)$ is the intensity value of the pixel at polar coordinates (x,y), $I_c(x,y)$ is the intensity value of the pixel at Cartesian coordinates (x,y), X and Y are the horizontal and vertical size of the desired output bitmap, R is the radius of the Petri dish, and (x_0,y_0) are the coordinates of the geometric center of the pattern. This transformation is performed by a computer program written *ad-hoc*.

B. General Experimental Conditions. All the experiments were designed to precipitate PbI_2, a reddish compound with a high value of specific gravity (6.16 g/cm^3). Its calculated thermodynamic solubility product is 8.49×10^{-9}.[16] PbI_2 precipitation was obtained by counterdiffusion of KI and $Pb(NO_3)_2$ solutions. Agarose L (Pharmacia), KI (Panreac), and $Pb(NO_3)_2$ (Panreac) were used as purchased without previous purification. All the solutions were made using bidistilled water. A typical experiment was carried out using the following procedure: the gelled solution of KI was prepared by mixing the appropriate amount of KI solution (1 mL) and agarose L (10 mg) to obtain an agarose concentration of 1% (w/v). The mixture was heated up to 90 °C (in a thermostated bath) under continuous stirring at reflux to reduce evaporation until a colorless and homogenous solution was obtained. Once a clear sol was obtained, aliquots of this solution, 50 μL each, were quickly poured into the capillary tubes (length 70 mm, diameter 1.5 mm). The bottoms of the capillary tubes were sealed with cyanoacrylate, and the solution was allowed to gel. The gelling temperature of agarose is 40 °C, and therefore the transfer has to be made quickly to avoid uncontrolled gelling behavior. After 30 min, this solution is gelled and a $Pb(NO_3)_2$ solution (50 μL)

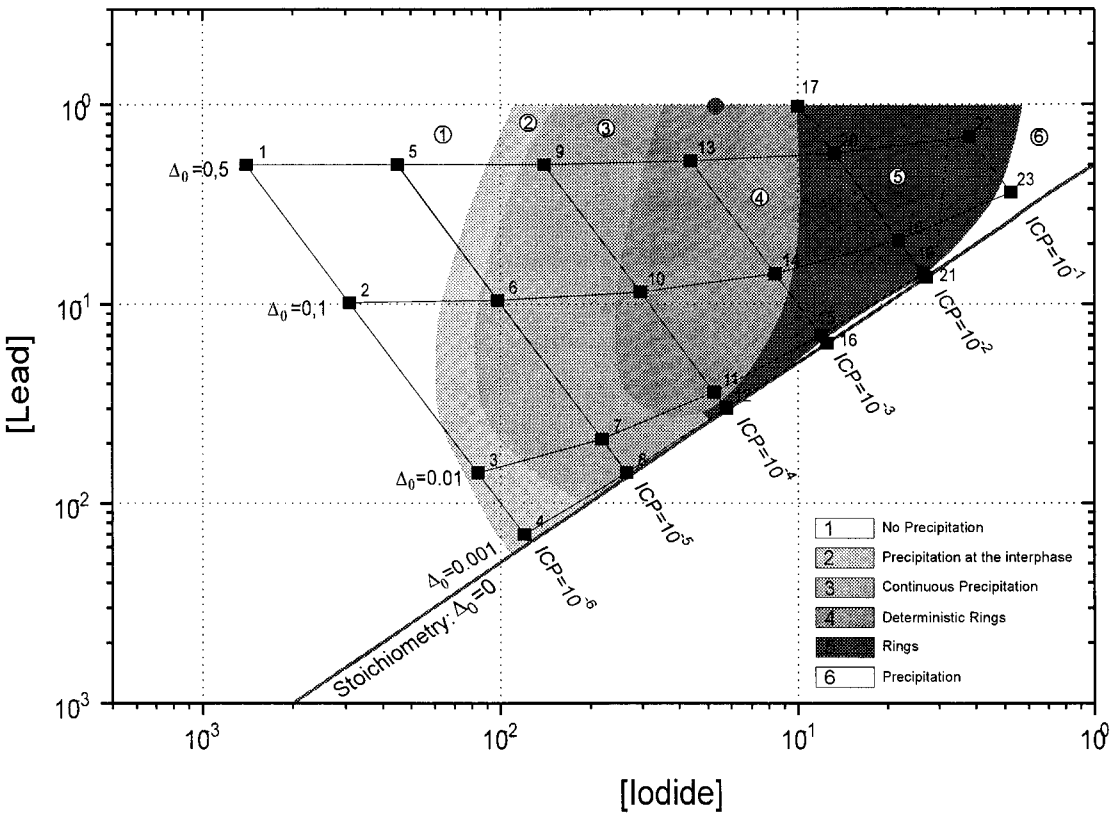

Figure 2. Pattern behavior of two counterdiffusing reacting solutions as a function of the starting stoichiometry of the reactants and starting supersaturation. Note that the formation of Liesegang patterns is just one possible morphological output of the system.

was poured onto the gel. The tubes were sealed with parafilm to avoid evaporation.

The first step of this study was devoted to find the behavior of patterning of the Liesegang systems as a function of the reactant concentration by performing a systematic screening of the starting conditions. The range of concentration used for KI solutions was from 0.0014 to 0.525 (M) and for the case of $Pb(NO_3)_2$ from 0.007 to 1.049 (M). The results of this study are extremely illustrative of the relation between stoichiometry, ICP ($[Pb(NO_3)_2][KI]^2$), and pattern formation (Figure 2). A general discussion of this study will be published elsewhere, but in relation to the aim of the present work we used it to choose the values for the starting concentration of reactants for which intermittent precipitation occurs and it does in a more deterministic way with better definition. These conditions, marked with a circle in Figure 2 ($[KI] = 0.05$ M and $[Pb(NO_3)_2] = 1$ M, ICP $= [I^-]^2[Pb^{+2}] = 2.5 \times 10^{-3}$), were used in our experimental study to test the influence of gravity.

The second step prior to testing the influence of gravity was the estimation of the reproducibility of the pattern. Ten identical experiments were performed in test tubes using the starting conditions mentioned above. The experiments were carried out at room temperature (24 ±1 ×bcC) and with the precipitation front advancing parallel to **g**. They yield a mean value for the kinetic coefficients $k_m = (X_{n+1} - X_n)/X_n$ of 0.119 with a standard deviation of 0.0034.

C. Experiments To Test the Effect of Gravity on the Kinetics of Pattern Formation. The same procedure described above was used to study the effect of gravity on the kinetics of Liesegang patterns. The PbI_2 pattern was obtained by counterdiffusion of KI and $Pb(NO_3)_2$ solutions at concentrations of 0.05 and 1.0 M, respectively. In these cases, both reacting solutions were gelled using agarose gel. The volume ratio of the KI and $Pb(NO_3)_2$ gels was kept equal to 1, except in the two-dimensional experiments in Petri dishes. The following tests were designed.

Test No. 1: Experiments with Rotating Tubes. Twenty identical test tubes (length = 100 mm, diameter = 10 mm) were prepared with the procedure described above using 1% agarose gel (w/v). These 20 tubes were randomly distributed in two sets of 10 tubes. The 10 tubes of the first set were placed on a circular holder, arranged with a radial distribution with a gap between them of 36°, and the holder was kept unrotated during the whole experiment. The banding formation in this case was achieved with 10 different orientations with respect to **g**. The 10 tubes of the second set were arranged in the same way in another holder with orbital rotation, and it was immediately switched on to start a rotation at 12 revolutions/min. Therefore, the Liesegang structures were obtained in all the tubes of the second set with the same average orientation with respect to **g**; see Figure 3a.

Test No. 2: Inverted Tubes. Ten identical test tubes (length = 100 mm, inner diameter = 10 mm) were prepared. All them were oriented vertically with the reaction front advancing parallel to gravity. Once six or seven bands appeared (which occurs after 2 h), five test tubes were inverted. We ended the experiments when a pattern with 12 or 13 bands was formed (after 25 h). The kinetics parameters of the two groups of test tubes were compared.

Test No. 3: Experiments with 1+1 Symmetry. This is a simple test which is performed in cassettes made of two glass plates placed apart from each other with a thin gap of 3 mm. Therefore, we get one-dimensional precipitation front initially located at the interface between the reactants. The internal dimensions of the gel cassettes were 8 × 4.5 cm^2 and the thickness of the gel layer was 3 mm. Four identical experiments were performed using an agarose concentration of 0.5% w/v. One cassette was allowed to stand in a vertical position with **g**

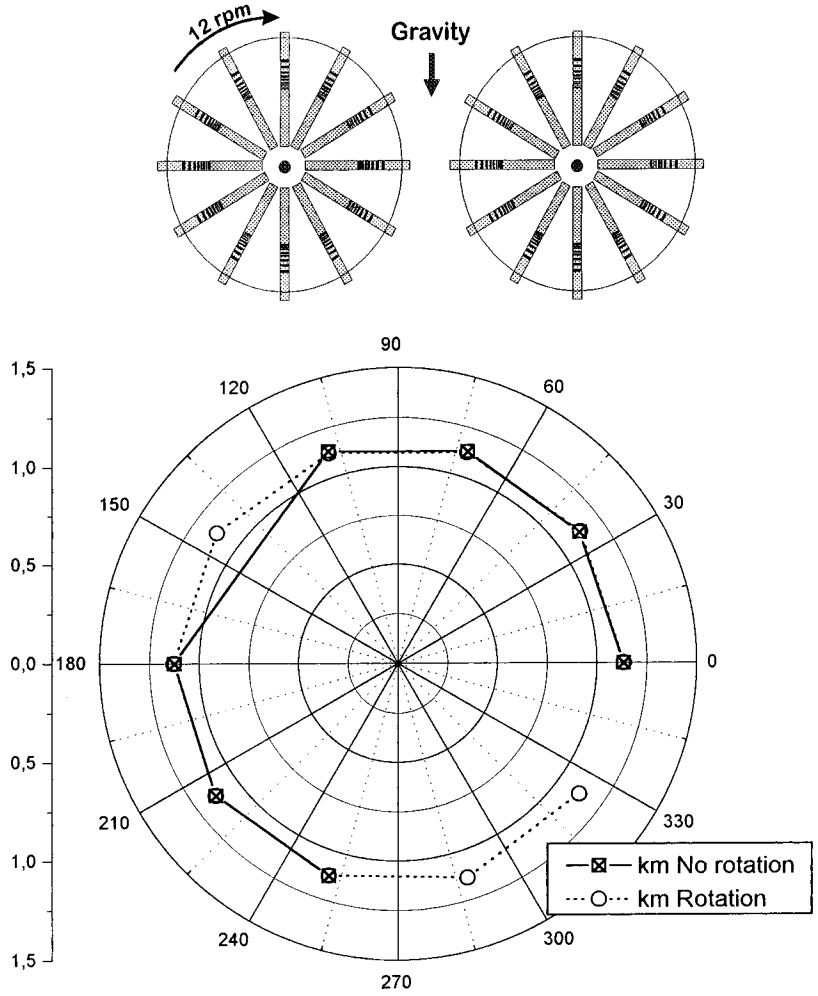

	Mean	sd	se	Sum	N
kp(R)	1,165	0,008	0,003	8,152	7
km(R)	1,132	0,003	0,001	7,926	7
km	1,131	0,005	0,002	11,314	10
kp	1,161	0,004	0,001	11,611	10

Figure 3. (a, top) Experimental arrangement used to perform the rotation test described in the text (test no. 1). (b, bottom) Polar plot showing the comparison between the values taken by the kinetics constants k_m and k_p for rotating and unrotating test tubes. For the sake of clarity, k_m+1 values have been used in the plot.

parallel to the advance of the precipitation front. A second cassette was maintained antiparallel, and the remaining two plates were oriented 45° clockwise and counterclockwise from **g**.

Test No. 4: Two-Dimensional Experiments. These were performed using a simple glass Petri dish with a diameter of 95 mm. A KI−agarose sol (35 mL) at 90 °C was poured into the dish. Once the thin KI layer was gelled, a disk of gel from the center of the dish was removed with the help of a mold. The cylindrical hole obtained was carefully filled with a hot sol of $Pb(NO_3)_2$−agarose (2.5 mL). With this arrangement the diffusion front has a radial geometry that advances, creating rings of increasing diameter. Ten experiments were carried out. Once the $Pb(NO_3)_2$ gel was settled, five Petri dishes were kept in a vertical position, and thus the reaction front advances scanning all the possible inclinations with respect to **g**. The other five dishes were oriented perpendicular to **g**. Two experimental sets were performed, one of them using 1% agarose (w/v) and the other one using 0.5% agarose (w/v).

III. Results and Discussion

In test 1 no significant deviation of the kinetic parameters in correlation with gravity was observed. The table in Figure 3b shows the values of the kinetics constants defined by Jablczynski,[17] $k_m = (X_{n+1} - X_n)/X_n$ and $k_p = (X_n/A)^{1/n}$, obtained for rotating and unrotating tubes. In Figure 3 we show a comparative graph for the values of the kinetics constant obtained at different **g** orientations in rotating and nonrotating tubes.

Test 2 was performed with the aim of detecting any difference when the front of precipitation advances parallel and antiparallel to the gravity field. This test was finished when 12 or 13 bands were formed. We did not observe any significant difference between the patterns. Figure 4 shows a typical plot of experimental data fitted to the Jablczynski expressions for a test tube inverted (antiparallel to **g**) after the seventh ring appears. The highlighted point corresponds to the last ring formed before the tube was inverted. Note that no significant deviation can be observed. In Figure 5 we show a comparative

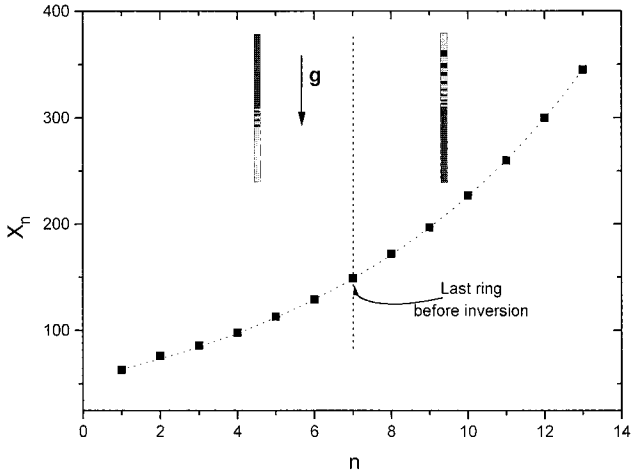

Figure 4. X_n versus n plot for a test tube that was inverted after the formation of the seventh ring (test no. 2). Note that the trend of the pattern formation remains identical after the inversion of the test tube.

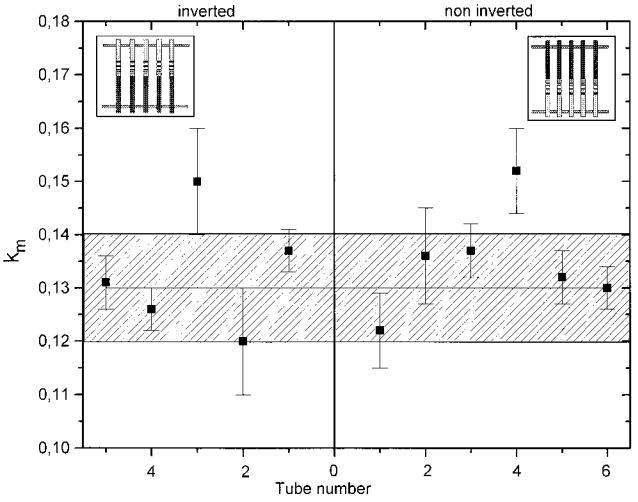

Figure 5. Values of k_m for six test tubes for which the precipitation front advances parallel to gravity and five test tubes for which the precipitation front advances antiparallel to gravity.

plot of k_m values obtained for inverted and noninverted tubes, as well as the test tubes number used in the analysis.

The third test (see Figure 6) shows that in all cases the degree of curvature of the precipitation front with respect to the initial interface between the two reacting gelled solutions does not depend on the orientation of the container.

The main disadvantage of the previous tests is that we need to compare experiments made in different test tubes, and therefore small differences in the starting conditions (temperature, reactant concentrations, hetereogenities of the test tubes, etc.) might produce undesirable changes in the pattern formation, making the test less accurate. The Petri dish test (test 4) was designed to avoid any plausible influence of small deviations between comparative experiments that could result in a lack of reproducibility. Note that, when the dish is oriented parallel to the **g** vector as shown in Figure 7a, all the different relative orientations of the precipitation front with respect to **g** are tested in one single experiment using the same gel. As can be observed in Figure 7b, when we used an agarose concentration of 1% (w/v), there was no difference in ring formation for different relative orientations of the precipitation front and the **g** vector, the pattern being a set of concentric rings centered in the $Pb(NO_3)_2$ gelled disk.

The settling velocity V_g of a particle of radius r_p and density ρ in a fluid of viscosity η and density ρ_0 is obtained by the

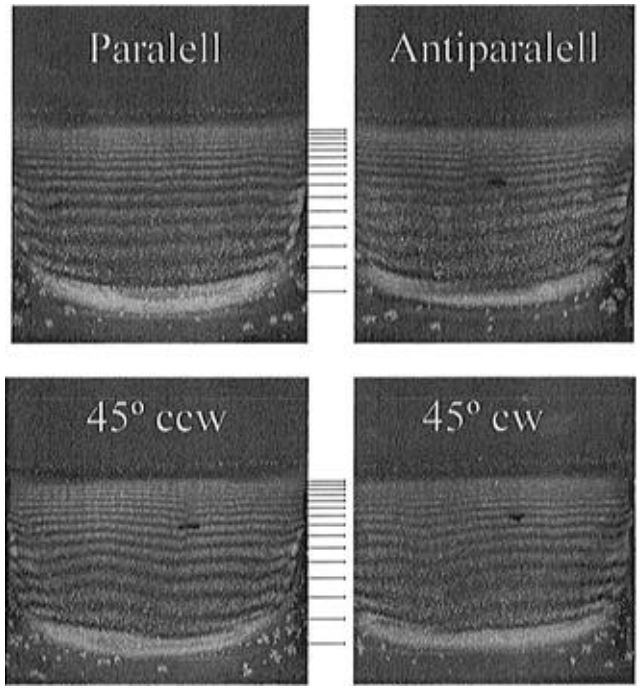

Figure 6. Liesegang pattern obtained using 1+1 symmetry for four different orientations with respect to gravity (test no. 3).

relation[18]

$$V_g^2 = \frac{8}{3}\frac{(1-c)^2(\rho-\rho_0)gr_p}{C_r\rho_0} \tag{3}$$

For very low Reynolds number *Re* (for instance smaller than 1 for a particle radius smaller than 55 μm) we can consider the drag coefficient C_r equal to 24/*Re*, and assuming no concentration dependence, that is $C = 0$, the above equation takes the simpler form

$$V_g = \frac{2r_p^2}{9\eta}(\rho-\rho_0)g \tag{4}$$

The effective pore size (diameter) of agarose gels at a concentration of 1% has been measured to be close to 1500 Å, fulfilling a concentration dependence of the type[19]

$$\bar{P} = kC^{-0.7} \tag{5}$$

with $k = 140.7$. Considering only geometrical effects, the largest particles that could settle in the gel framework are those with a radius r_p smaller than 700 Å. Using eq 4 with $\rho_0 = 1$ gr/cm, $\rho = 6.16$ gr/cc, and $\eta = 0.01$P, we calculate the gravitational drift in μm/h for PbI_2 particles of different size, which is shown in Figure 8. Note that for particles with a radius of 700 Å the settling velocity is about 200 μm/h. Considering that we have measured the formation of a ring in less than 2 min, the gravitational drift during the characteristic time of the pattern formation is ca. 6.6 μm. It should be noted that the settling velocities shown in Figure 8 are actually slower because (a) they were calculated for the settling of a spherical particle in cylindrical pores of uniform size, which is an unrealistic assumption as the pore structure is corrugated and the crystal shape is anisotropic; (b) the above simple model describes the settling of a single particle, but a realistic approach has to consider a finite concentration of particles where repulsive and

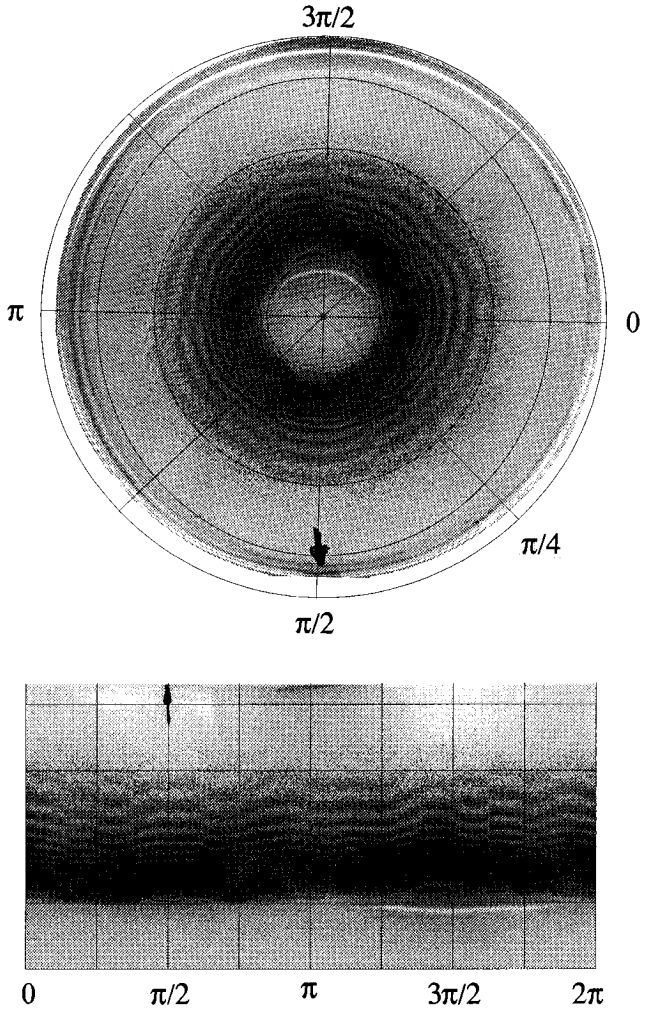

Figure 7. (a, top) Liesegang pattern obtained using agarose at a concentration of 1% (w/v). (b, bottom) Cartesian coordinates (x,y) obtained from the polar coordinates obtained from the image shown in part a.

attractive forces between them and the gel matrix occur. The existence of repulsion or attraction forces between two particles is related to their dielectric function and that of the fluid media.

It should be underlined that our tests are able to record the effect of gravity when it exists. Because of the higher reliability of this Petri dish test, we also performed another set of experiments using agarose at a concentration of 0.5% (w/v). At this concentration the effective pore size increases to r_p = 1200 Å, and as shown in Figure 8, a shift of more than 2 mm is expected for time periods as low as 10 h. When the test is carried out, a clear effect of the gravity field can be observed with an up to 3 mm gravity-provoked shift that breaks the radial symmetry of the Liesegang pattern (Figure 9). It is important to note that while the agarose concentration plays the main role in the control of the gravity effect, the waiting time to perform the experiments should also be taken into account. For instance, the effect of gravity is reduced or even removed by aging 4 days the KI gelled solution. It occurs because of the loss of water by evaporation and aging the gel. This was checked by recording the development in time of the absorption values at 750 nm by UV−visible spectroscopy. At time 0, after mixing the components the measured value was 0.013 which changes to 0.059 after 50 min (corresponding to a well-settled gel) and changes to 0.064 after 4 days. Therefore, to reproduce the above experiment, not only the agarose concentration but also the age of the gel have to be considered.

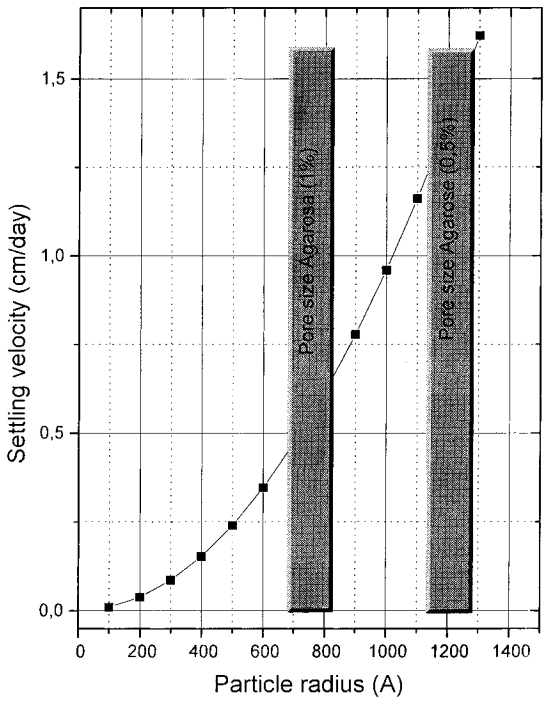

Figure 8. Settling velocity of PbI_2 particles as a function of particle size. The calculations are made for a single particle and low Reynolds number. For comparison, the bars show the calculated pore size for agarose gels at concentrations of 1% and 0.5%.

Moreover, the influence of gravity is also detected when only one of the reactants is gelled. Figure 10a shows the result of the experiments performed using a gelled solution of KI at 0.05 M concentration and a $Pb(NO_3)_2$ solution at 1 M concentration as the top solution. During the formation of the pattern, no differences were observed when the front advanced parallel or antiparallel to the gravity vector. For instance, the mean value of k_m for experiments parallel to **g** was 0.132 ± 0.008, while that for experiments performed antiparallel to **g** was 0.140 ± 0.005. However, once the first formed bands start to dissolve, the effect of gravity becomes clear. We have been able to measure different values of the rate of dissolution of rings for capillary tubes kept parallel and antiparallel to **g**. As an example, Figure 10b shows the patterns as observed after 3 days, where it is clearly observed that the dissolution rate is greater for capillaries kept with the Pb^{2+} solution on top of the gelled KI solution. This observation will be discussed elsewhere in detail.

IV. Conclusions

The results obtained in this study suggest that the kinetics of the formation of Liesegang structures is unaffected by the gravity field when they are produced in gelled media. This invariance with **g** is supported by the evaluation of the sedimentation rate of particles smaller than the pore size in a gelled medium for the characteristic time of formation of the rhythmic precipitation pattern. In any case, the sensitivity of the Liesegang patterns to small variations in the initial conditions (reactant concentrations, pH, gel porosity, gel homogeneity, geometry of the reservoir and geometry of the reactant sources, cleanness, etc.) produces deviations in two "identical" experiments which may mask an eventual small effect of gravity. Obviously, gravity could affect the experimental results (a) when the experiments are performed in a gel-free medium; (b) when using gels with a quasi unimodal pore size distribution and average pore size larger than tenths of microns; and (c) when the crystal mass is

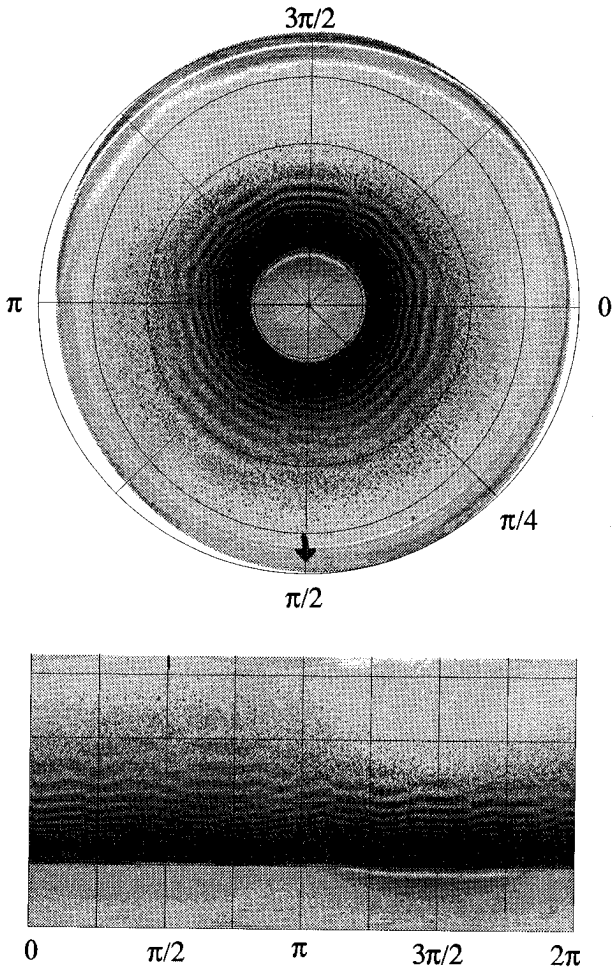

Figure 9. (a, top) Liesegang pattern obtained using agarose at a concentration of 0.5% (w/v). (b, bottom) Cartesian coordinates (*x*,*y*) obtained from the polar coordinates of the image shown in part a. Unlike for the case of agarose gels at a concentration of 1% (w/v) shown in Figure 7, note how in this case the effect of gravity can be observed.

large enough to overcome the elasticity modulus of the gel structure. Therefore, to design a microgravity-conducted experiment with the unique aim of the evaluation of the kinetics of pattern formation does not seem worthwhile. However, it is expected that the deviations from linearity observed when gels are used to avoid convection will be considerably reduced if the experiments are carried out in gel-free media under microgravity.

There is another powerful reason to perform experiments leading to Liesegang structures under gravity-free conditions. Under certain circumstances, the difference in size among the crystals forming the different bands can be at least 4 orders of magnitude. Therefore, the possibility of breaking the pattern by gravity-driven convection increases as the structure advances. If we remember that Liesegang banding is a type of nonequilibrium structure, to maintain such a structure in a gel-free medium in time could provide an estimation of the stability of the gravity field and the number of bands that we will be able to maintain could be used to estimate the time homogeneity of the microgravity conditions.

Acknowledgment. We gratefully acknowledge financial support from ESA and Spanish CICYT through Project PB93-1137. We also thank the assistance of Miss Eva Herrera in the laboratory work. D.R. acknowledges grants from the Ministerio de Educación y Ciencia (Spain) and F.O. a grant from Junta de Andalucía (Spain).

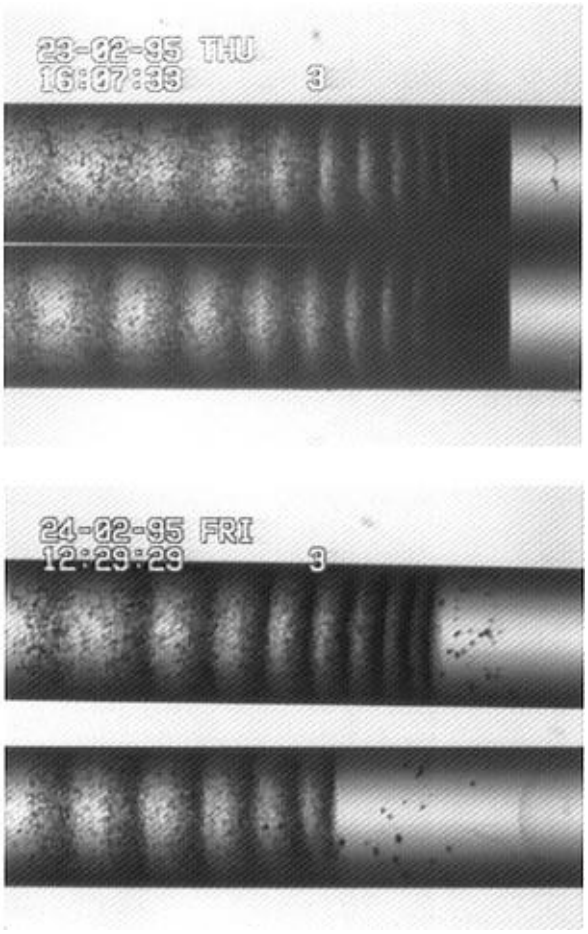

Figure 10. (a, top) Liesegang pattern obtained after 2 h for a system where the iodide source is gelled with agarose while the lead source is a gel-free water solution (upper, pattern obtained antiparallel to **g**; botton, pattern obtained parallel to **g**). (b, bottom) The same pattern after 20 h.

References and Notes

(1) Liesegang, R. E. *Naturwiss. Wochenschr*. **1896**, *11*, 353; *Phot. Archiv.* **1896**, *21*, 221.
(2) Henisch, H. K. *Periodic Precipitation*; Pergamon Press: Oxford, 1991.
(3) Bewersdorff, A.; Borckmans, P.; Muller, S. C. In *Fluid Sciences and Materials Sciences in Space*; Walter, H. U., Ed.; Springer Verlag: Berlin, 1987.
(4) Lovett, R.; Ortoleva, P., Ross, J. *J. Chem. Phys*. **1978**, *69*, 947.
(5) Venzl, G., Ross, J. *J. Chem. Phys*. **1982**, *77*, 1302.
(6) Davies, E. C. H. *J. Am. Chem. Soc*. **1922**, *44*, 2698.
(7) Hedges, E. S. *Liesegang Rings and Other Periodic Structures*; Chapman & Hall: London, 1932.
(8) Kai, S.; Müller, S. C.; Ross, J. *J. Chem. Phys*. **1982**, *76*, 1392.
(9) Das, I.; Das, S. S.; Pushkarna, A., Chand, S. J. *Colloid. Interface Sci*. **1989**, *130*, 176.
(10) Das, I.; Pushkarna, A.; Bhattacharjee, A. *J. Phys. Chem*. **1990**, *94*, 8968.
(11) Zrínyi, M.; Gálfi, L.; Smidróczki, É.; Rácz, Z.; Horkay, F. *J. Phys.Chem*. **1991**, *95*, 1618.
(12) Foster, A. W. *J. Phys. Chem*. **1919**, *23*, 645.
(13) Burton, E. F.; Bell, X. *J. Phys. Chem*. **1921**, *25*, 526.
(14) Das, A.; Pushkarna, A.; Agrawal, N. R. *J. Phys. Chem*. **1989**, *93*, 7269.
(15) Kisch, B. *Kolloid-Z*. **1929**, *49*, 154.
(16) *Handbook of Chemistry and Physics*, 71st ed; David R. Lide, D. R., Ed.; CRC Press: Boston, 1990−1991; pp 8−39.
(17) Jablczynski, M. *Bull. Soc. Chem. Fr*. **1923**, *33*, 1592.
(18) Allen, J. R. L. *Principles of Physical Sedimentology*; George Allen and Unwin: London, 1985; pp 39−53.
(19) Righetti, P. G.; Brost, B. C. W.; Snyder, R. *J. Biochem. Biophys. Methods* **1981**, *4* , 347.

JP953351M